ChemComm

COMMUNICATION

View Article Online
View Journal | View Issue

Cite this: *Chem. Commun.*, 2023, 59, 1165

Received 23rd November 2022,
Accepted 14th December 2022

DOI: 10.1039/d2cc06345j

rsc.li/chemcomm

syn-Elimination of glutamylated threonine in lanthipeptide biosynthesis†

Raymond Sarksian,[a] Lingyang Zhu[b] and Wilfred A. van der Donk*[ac]

Methyllanthionine (MeLan) containing macrocycles are key structural features of lanthipeptides. They are formed typically by *anti*-elimination of L-Thr residues followed by cyclization of L-Cys residues onto the (*Z*)-dehydrobutyrine (Dhb) intermediates. In this report we demonstrate that the biosynthesis of lanthipeptides containing the D-*allo*-L-MeLan macrocycle such as the morphogenetic lanthipeptide SapT proceeds through (*E*)-Dhb intermediates formed by net *syn*-elimination of L-Thr.

Lanthipeptides are peptidic natural products defined by the presence of lanthionine (Lan) and/or methyllanthionine (MeLan) residues and represent a large class of ribosomally synthesized and post-translationally modified peptides (RiPPs).[1] One of the most common posttranslational modifications (PTMs) in RiPPs is macrocyclization.[2–7] Macrocyclic peptides often increase stability towards proteolytic degradation and display more potent bioactivities compared to their linear counterparts.[8]

Macrocyclization for lanthipeptides occurs by thiol-Michael addition of L-Cys to electrophilic dehydroalanine (Dha)/dehydrobutyrine (Dhb) intermediates that are formed by net dehydration of Ser/Thr residues.[1,5,9] In class I lanthipeptide biosynthesis the dehydration reaction is catalyzed by a LanB enzyme that first activates the side chain of Ser/Thr residues through a transesterification reaction using Glu-tRNA^{Glu} (Fig. 1A).[10–13] Glutamate elimination by the LanB enzyme in a separate active site then generates Dha/Dhb residues (Fig. 1A). Split LanB enzymes have been reported where the glutamyl transferase and glutamyl lyase (GL) domains are separate polypeptides.[14–18] The cyclization process for lanthipeptides can generate up to two Lan and four MeLan diastereomers.[1,18,19] The cyclization reaction is catalyzed by a LanC cyclase for class I lanthipeptides (Fig. 1A).[1,20] The (*2S*,*6R*)- and (*2R*,*6R*)-Lan diastereomers, hereafter referred to as DL- and LL-Lan, have been detected in lanthipeptides, and three out of four possible MeLan stereoisomers have been observed, (*2S*,*3S*,*6R*)-, (*2R*,*3R*,*6R*)-, and (*2S*,*3R*,*6R*)-MeLan, hereafter denoted as DL-, LL-, and D-*allo*-L-MeLan (Fig. 1B).[18,19,21–25]

Dehydration of L-Thr residues yields (*Z*)-Dhb in all characterized lanthipeptides (Fig. 1C). DL- and LL-MeLan diastereomers are believed to form by *anti*-addition of L-Cys across (*Z*)-Dhb intermediates; addition across the *Si* face results in DL-MeLan, whereas addition across the *Re* face gives LL-MeLan.[1,21,23] DL-MeLan has been historically observed for most lanthipeptides including nisin,[26] whereas LL-MeLan has been detected only in the past decade, particularly in substrate-controlled cyclizations.[23,27] D-*allo*-L-MeLan macrocycles were recently discovered in the morphogenetic lanthipeptide SapT (Fig. 2A).[18] D-*allo*-L-MeLan could be formed through *anti*-elimination of L-Thr residues to yield a (*Z*)-Dhb intermediate followed by *syn*-addition of L-Cys across the *Re* face of the (*Z*)-Dhb intermediate.[18] Alternatively, D-*allo*-L-MeLan can be generated through net *syn*-elimination of L-Thr residues to generate an (*E*)-Dhb intermediate followed by *anti*-addition of L-Cys across the *Si* face of the (*E*)-Dhb intermediate.[18] A lanthipeptide cyclase has yet to be characterized that catalyzes *syn*-addition and (*E*)-Dhb residues have yet to be observed for a RiPP. In this report we differentiate between these two mechanistic possibilities by characterization of a model biosynthetic intermediate containing a Dhb residue generated by the SapT biosynthetic machinery.

The class I lanthipeptide SapT is produced from the *spt* biosynthetic gene cluster (BGC) that encodes the SptA precursor peptide, a split dehydratase consisting of SptB$_a$ and SptB$_b$, and the SptC cyclase (Fig. 2A).[18] SptB$_a$ is a glutamyl transferase and SptB$_b$ functions as a GL that catalyzes glutamate elimination

[a] *Department of Chemistry and Howard Hughes Medical Institute, University of Illinois at Urbana-Champaign, Urbana, IL, 61822, USA. E-mail: vddonk@illinois.edu; Tel: +1 217 244 5360*
[b] *School of Chemical Sciences NMR Laboratory, University of Illinois at Urbana-Champaign, Urbana, IL, 61822, USA*
[c] *Carl R. Woese Institute for Genomic Biology, University of Illinois at Urbana-Champaign, Urbana, IL, 61822, USA*

† Electronic supplementary information (ESI) available: Experimental procedures and supplementary figures and tables. See DOI: https://doi.org/10.1039/d2cc06345j

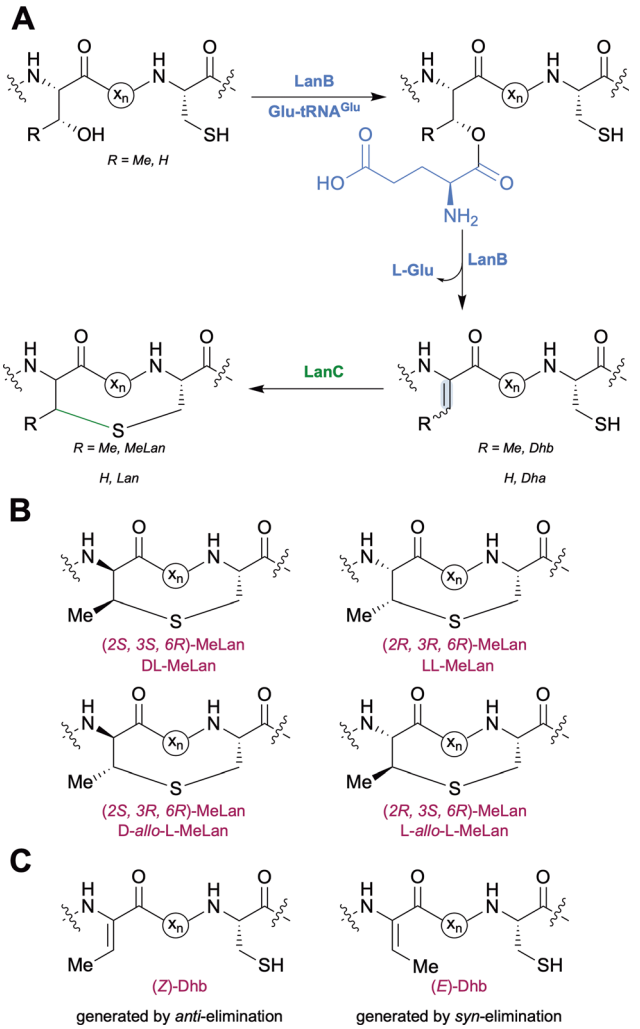

Fig. 1 (A) Class I lanthipeptide biosynthesis. (B) Four MeLan stereoisomers. (C) MeLan residues can be generated from either (*Z*)- or (*E*)-Dhb intermediates.

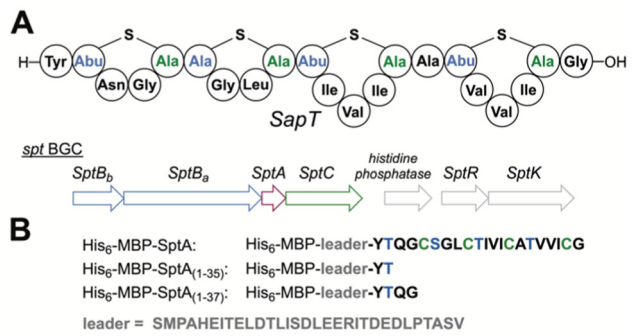

Fig. 2 (A) Schematic structure of SapT and associated BGC. Abu, 2-aminobutyric acid. For full structures of the crosslinks, see Fig. 1. (B) Design of truncated His_6-MBP fusion peptides used for heterologous production in this study.

(Fig. 2A). Bioinformatic and sequence analysis previously revealed that the putative active site of $SptB_b$ contains amino acid residues that are different from crystallographically characterized class I GLs that catalyze *anti*-elimination.[18,19]

The biosynthetic pathway for SapT was previously reconstituted in *Escherichia coli*,[18] and we used this approach in this study to obtain sufficient amounts of a Dhb-containing intermediate for structural characterization. To simplify analysis, the SptA precursor peptide was truncated by site-directed mutagenesis to prepare a substrate that would generate just a single Dhb residue and that did not contain any Cys residues to avoid cyclization (Fig. 2B). Two peptides were generated, $SptA_{(1–37)}$ and $SptA_{(1–35)}$, both fused to the C-terminus of maltose binding protein (MBP). Co-expression of these peptides with $SptB_a$ and $SptB_b$, as well as glutamyl-tRNA synthase (GluRS) and $tRNA^{Glu}$ from *Thermobispora bispora* in *E. coli* followed by isolation by metal affinity chromatography and proteolytic removal of the His_6-MBP tag revealed dehydration of $SptA_{(1–37)}$ to form $mSptA_{(1–37)}$ (for modified $SptA_{(1–37)}$) as the major product with unreacted $SptA_{(1–37)}$ as a minor product (Fig. 3 bottom spectrum, and Table S1, ESI†). Glutamylation but not glutamate elimination was observed for $SptA_{(1–35)}$ that contains a C-terminal Thr. The lack of elimination activity may either be the result of decreased affinity of $SptB_b$ for the glutamylated peptide when situated at the C-terminus, or it may be the result of the decreased acidity of the α-C–H bond in a C-terminal Thr residue that is adjacent to a carboxylate rather than an amide (Fig. 3, Table S1, ESI†).[28] GLs have been shown to be highly tolerant with respect to the leaving group,[29] and hence the increased pK_a may be the most likely explanation. Regardless, we focused only on $mSptA_{(1–37)}$ for the remainder of the study.

$mSptA_{(1–37)}$ was digested with trypsin to remove the N-terminal portion of the peptide. The C-terminal digestion fragment ($mSptA_{(1–37)trypsin}$) was characterized by liquid chromatography (LC) interfaced with mass spectrometry (MS). High-resolution and tandem MS confirmed the dehydration state and localized the Dhb residue to position 35 of $mSptA_{(1–37)}$ (Fig. 4A and B and Table S2, ESI†) as expected since the other

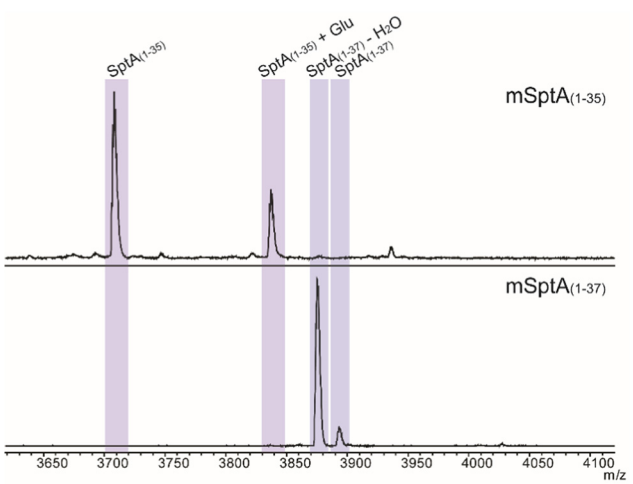

Fig. 3 Matrix-assisted laser desorption ionization time-of-flight (MALDI-TOF) mass spectrometry analysis of truncated SptA peptides coexpressed with $SptB_a$, $SptB_b$, and $tRNA^{Glu}$ and GluRS from *T. bispora*.

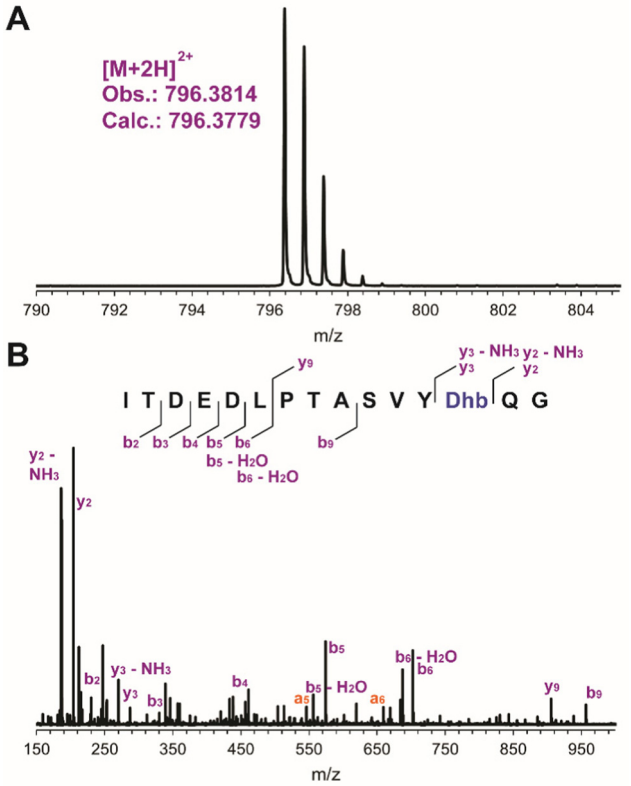

Fig. 4 LC-MS analysis of the C-terminal trypsin digestion fragment from $mSptA_{(1-37)}$ containing a single Dhb residue. (A) High-resolution electrospray ionization MS (ESI-MS) analysis. (B) Tandem ESI-MS analysis, observed a ions are shown in orange but not labeled on the peptide.

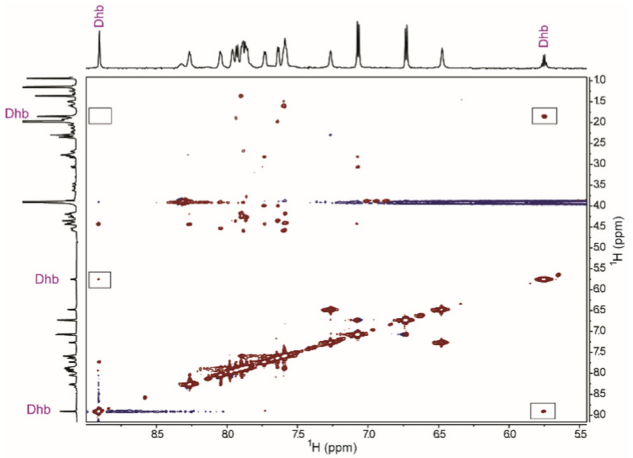

Fig. 5 Characteristic region of the $^1H-^1H$ NOESY spectrum of $mSptA_{(1-37)trypsin}$. Boxes are used to highlight presence and absence of key NOE signals for determining the Dhb geometry.

Ser/Thr residues are part of the SptA leader peptide and are not modified during the biosynthesis of SapT (Fig. 2B).

Next, $mSptA_{(1-37)trypsin}$ was produced on a larger scale for characterization of the alkene geometry by nuclear magnetic resonance (NMR) spectroscopy. One dimensional ^1H NMR spectra and two-dimensional homonuclear ^1H-^1H TOCSY (total correlation spectroscopy) and NOESY (nuclear Overhauser effect spectroscopy) data were acquired for chemical shift assignment of all resonances (Table S3 and Fig. S1–S4, ESI†). The ^1H NMR spectrum of $mSptA_{(1-37)trypsin}$ in 70% acetonitrile-d_3/30% H_2O revealed distinct resonance frequencies for the Dhb residue (Fig. S1 and Table S3, ESI†). The most downfield singlet at 8.90 ppm was identified as the Dhb amide proton, and a distinct quartet was observed at 5.75 ppm for the vinylic proton of the Dhb residue. Only a single set of Dhb-derived signals was detected, consistent with the MS-MS data suggesting that only Thr35 was dehydrated in $mSptA_{(1-37)}$. The vinylic proton is coupled to the allylic methyl group of the Dhb residue at 1.85 ppm that is present as the expected doublet. An NOE signal was observed between the vinylic proton and methyl protons of the Dhb residue, as well as a distinct NOE signal between the vinylic proton of the Dhb residue and the amide proton of the same residue (Fig. 5 and Fig. S4, ESI†), revealing the spatial vicinity of the vinylic and the amide protons of the Dhb residue. An NOE signal was not observed between the methyl group and amide proton of the Dhb residue (Fig. 5 and Fig. S4, ESI†). The observed NOEs differ significantly from what is observed for (*Z*)-Dhb residues in previously characterized lanthipeptides[30,31] (Fig. S5 and S6, ESI†) and linaridins.[32,33] Although we cannot rule out that during purification minor products may have been removed that could contain (*Z*)-Dhb, these results clearly demonstrate that the predominant product of $mSptA_{(1-37)trypsin}$ contains an (*E*)-Dhb and not a (*Z*)-Dhb residue. To our knowledge, this represents the first example of detection of a peptide containing an (*E*)-Dhb residue with ribosomal origin. Cypemycin had been proposed to contain an (*E*)-Dhb, but that proposal was recently shown to be incorrect.[32] Therefore, the GL $SptB_b$ in SapT biosynthesis catalyzes net *syn*-elimination of glutamylated Thr residues to form (*E*)-Dhb residues. Subsequent *anti*-addition of L-Cys across the *Si* face of the (*E*)-Dhb residue by SptC then forms D-*allo*-L-MeLan macrocycles found in SapT. Whether the formation involves a concerted *syn*-elimination reaction or potentially an $E1_{cb}$ mechanism is currently not known. It is intriguing, however, that neither sequence alignments nor a homology model of $SptB_b$ identified a residue that may stabilize the enolate intermediate that would be formed in an $E1_{cb}$ mechanism.[19] We cannot rule out however that amide backbone hydrogens might stabilize the build-up of negative charge on the oxygen of the enolate through hydrogen bonding interactions as often seen in proteases.[34]

The characterization of a model biosynthetic intermediate containing an (*E*)-Dhb generated by $SptB_b$ provides a direct link between the stereochemistry of the Dhb intermediate and bioinformatic signatures that are observed for *syn*-GLs that differ from *anti*-GLs.[18,19] For the gene clusters that have been investigated thus far that contain a *syn*-GL (*spt* and *coi*), it is intriguing to note that the products contain D-*allo*-L-MeLan cross-links, but not (*E*)-Dhb residues.[18,19] Whether this will hold true for other lanthipeptides containing D-*allo*-L-MeLan cross-links with *syn*-GLs in the corresponding BGCs, which

constitute nearly one-fifth of all class I lanthipeptide BGCs, remains to be determined.

This study was designed by R. S and W. A. V. Experiments were performed by R. S. L. Z. assisted in NMR experiment setup. All authors contributed to data analysis and interpretation. R. S. and W. A. V. wrote the paper. All authors have given approval to the final version of the manuscript.

This work was supported by the National Institutes of Health (GM 058822). The authors thank Dr M. A. Simon for assistance with LC-MS and Prof. S. Nair and Dr Z.-F. Pei for sharing the data shown in Fig. S6 (ESI†). A Bruker MALDI TOF/TOF mass spectrometer was purchased with a grant from the National Institutes of Health (S10 RR027109 A). This study is subject to HHMI's Open Access to Publications policy. HHMI laboratory heads have previously granted a nonexclusive CC BY 4.0 license to the public and a sublicensable license to HHMI in their research articles. Pursuant to those licenses, the author-accepted manuscript of this article can be made freely available under a CC BY 4.0 license immediately upon publication.

Conflicts of interest

There are no conflicts to declare.

References

1 L. M. Repka, J. R. Chekan, S. K. Nair and W. A. van der Donk, *Chem. Rev.*, 2017, **117**, 5457–5520.
2 A. W. Truman, *Beilstein J. Org. Chem.*, 2016, **12**, 1250–1268.
3 M. Montalbán-López, T. A. Scott, S. Ramesh, I. R. Rahman, A. J. van Heel, J. H. Viel, V. Bandarian, E. Dittmann, O. Genilloud, Y. Goto, M. J. Grande Burgos, C. Hill, S. Kim, J. Koehnke, J. A. Latham, A. J. Link, B. Martínez, S. K. Nair, Y. Nicolet, S. Rebuffat, H.-G. Sahl, D. Sareen, E. W. Schmidt, L. Schmitt, K. Severinov, R. D. Süssmuth, A. W. Truman, H. Wang, J.-K. Weng, G. P. van Wezel, Q. Zhang, J. Zhong, J. Piel, D. A. Mitchell, O. P. Kuipers and W. A. van der Donk, *Nat. Prod. Rep.*, 2021, **138**, 130–239.
4 J. Lu, Y. Li, Z. Bai, H. Lv and H. Wang, *Nat. Prod. Rep.*, 2021, **38**, 981–992.
5 H. Lee and W. A. van der Donk, *Annu. Rev. Biochem.*, 2022, **91**, 269–294.
6 G. Zhao, D. Kosek, H. B. Liu, S. I. Ohlemacher, B. Blackburne, A. Nikolskaya, K. S. Makarova, J. Sun, C. E. Barry Iii, E. V. Koonin, F. Dyda and C. A. Bewley, *J. Am. Chem. Soc.*, 2021, **143**, 8056–8068.
7 K. A. Clark, L. B. Bushin and M. R. Seyedsayamdost, *ACS Bio. Med. Chem. Au*, 2022, **2**, 328–339.
8 A. Zorzi, K. Deyle and C. Heinis, *Curr. Opin. Chem. Biol.*, 2017, **38**, 24–29.
9 T. Le, K. Jeanne Dit Fouque, M. Santos-Fernandez, C. D. Navo, G. Jiménez-Osés, R. Sarksian, F. A. Fernandez-Lima and W. A. van der Donk, *J. Am. Chem. Soc.*, 2021, **143**, 18733–18743.
10 N. Garg, L. M. Salazar-Ocampo and W. A. van der Donk, *Proc. Natl. Acad. Sci. U. S. A.*, 2013, **110**, 7258–7263.
11 M. A. Ortega, Y. Hao, Q. Zhang, M. C. Walker, W. A. van der Donk and S. K. Nair, *Nature*, 2015, **517**, 509–512.
12 M. A. Ortega, Y. Hao, M. C. Walker, S. Donadio, M. Sosio, S. K. Nair and W. A. van der Donk, *Cell Chem. Biol.*, 2016, **23**, 370–380.
13 I. R. Bothwell, D. P. Cogan, T. Kim, C. J. Reinhardt, W. A. van der Donk and S. K. Nair, *Proc. Natl. Acad. Sci. U. S. A.*, 2019, **116**, 17245–17250.
14 K. I. Mohr, C. Volz, R. Jansen, V. Wray, J. Hoffmann, S. Bernecker, J. Wink, K. Gerth, M. Stadler and R. Müller, *Angew. Chem., Int. Ed.*, 2015, **54**, 11254–11258.
15 G. A. Hudson, Z. Zhang, J. I. Tietz, D. A. Mitchell and W. A. van der Donk, *J. Am. Chem. Soc.*, 2015, **137**, 16012–16015.
16 Y. Du, Y. Qiu, X. Meng, J. Feng, J. Tao and W. Liu, *J. Am. Chem. Soc.*, 2020, **142**, 8454–8463.
17 A. A. Vinogradov, M. Shimomura, N. Kano, Y. Goto, H. Onaka and H. Suga, *J. Am. Chem. Soc.*, 2020, **142**, 13886–13897.
18 R. Sarksian, J. D. Hegemann, M. A. Simon, J. Z. Acedo and W. A. van der Donk, *J. Am. Chem. Soc.*, 2022, **144**, 6373–6382.
19 R. Sarksian and W. A. van der Donk, *ACS Chem. Biol.*, 2022, **17**, 2551–2558.
20 B. Li, J. P. Yu, J. S. Brunzelle, G. N. Moll, W. A. van der Donk and S. K. Nair, *Science*, 2006, **311**, 1464–1467.
21 W. Tang and W. A. van der Donk, *Nat. Chem. Biol.*, 2013, **9**, 157–159.
22 C. T. Lohans, J. L. Li and J. C. Vederas, *J. Am. Chem. Soc.*, 2014, **136**, 13150–13153.
23 W. Tang, G. Jiménez-Osés, K. N. Houk and W. A. van der Donk, *Nat. Chem.*, 2015, **7**, 57–64.
24 J. Z. Acedo, I. R. Bothwell, L. An, A. Trouth, C. Frazier and W. A. van der Donk, *J. Am. Chem. Soc.*, 2019, **141**, 16790–16801.
25 I. R. Bothwell, T. Caetano, R. Sarksian, S. Mendo and W. A. van der Donk, *ACS Chem. Biol.*, 2021, **16**, 1019–1029.
26 J. L. Morell and E. Gross, *J. Am. Chem. Soc.*, 1973, **95**, 6480–6481.
27 W. Tang, G. N. Thibodeaux and W. A. van der Donk, *ACS Chem. Biol.*, 2016, **11**, 2438–2446.
28 T. L. Amyes and J. P. Richard, *Synlett*, 2017, 2407–2421.
29 A. A. Vinogradov, M. Nagano, Y. Goto and H. Suga, *J. Am. Chem. Soc.*, 2021, **143**, 13358–13369.
30 Z.-F. Pei, L. Zhu, R. Sarksian, W. A. van der Donk and S. K. Nair, *J. Am. Chem. Soc.*, 2022, **144**, 17549–17557.
31 S. C. Bobeica, L. Zhu, J. Z. Acedo, W. Tang and W. A. van der Donk, *Chem. Sci.*, 2020, **11**, 12854–12870.
32 L. Chu, J. Cheng, C. Zhou, T. Mo, X. Ji, T. Zhu, J. Chen, S. Ma, J. Gao and Q. Zhang, *ACS Chem. Biol.*, 2022, DOI: **10.1021/acschembio.1022c00657**.
33 Z. Shang, J. M. Winter, C. A. Kauffman, I. Yang and W. Fenical, *ACS Chem. Biol.*, 2019, **14**, 415–425.
34 L. Hedstrom, *Chem. Rev.*, 2002, **102**, 4501–4524.

